Inorganic Chemistry

Article

pubs.acs.org/IC

Supramolecular 2D/3D Isomerism in a Compound Containing Heterometallic $Cu^{II}_2Co^{II}$ Nodes and Dicyanamide Bridges

Saptarshi Biswas,[†] Carlos J. Gómez-García,[‡] Juan M. Clemente-Juan,[‡] Samia Benmansour,[‡] and Ashutosh Ghosh*,[†]

[†]Department of Chemistry, University College of Science, University of Calcutta, 92, A.P.C. Road, Kolkata-700 009, India

[‡]Instituto de Ciencia Molecular (ICMol), Universidad de Valencia, C/Catedrático José Beltrán 2. 46980 Paterna, Valencia, Spain

Supporting Information

ABSTRACT: Three new heterometallic copper(II)−cobalt(II) complexes $[(CuL^2)_2Co\{dca\}_2]\cdot H_2O$(**1**), $[(CuL^1)_2Co\{dca\}_2]_n$ (**2a**), and $[(CuL^1)_2Co\{dca\}_2]_n$ (**2b**) [dca^- = dicyanamide = $N(CN)_2^-$] have been synthesized by reacting the "metallo-ligand" [CuL^1] or [CuL^2] with cobalt(II) perchlorate and sodium dicyanamide in methanol−water medium (where H_2L^1 = *N,N′*-bis(salicylidene)-1,3-propanediamine and H_2L^2 = *N,N′*-bis(α-methylsalicylidene)-1,3-propanediamine). The three complexes have been structurally and magnetically characterized. Complex **1** is a discrete trinuclear species in which two metallo-ligands coordinate to a cobalt(II) ion through the phenoxido oxygen atoms along with two terminally coordinated dicyanamide ions. On the other hand, complexes **2a** and **2b** are one of the very scarce examples of supramolecular isomers since they present the same $[(CuL^1)_2Co\{dca\}_2]$ trinuclear units (very similar to the trinuclear core in **1**) and differ only in their superstructures. Thus, although each Cu_2Co trimer in **2a** and **2b** is connected to four other Cu_2Co trimers through four $\mu_{1,5}$-dca^- bridges, **2a** presents a square two-dimensional structure (each Cu_2Co trimer is connected to four in-plane Cu_2Co trimers); whereas, **2b** shows a triangular three-dimensional lattice (each Cu_2Co trimer is connected to three in-plane and one out-of-plane trimers). Variable-temperature magnetic susceptibility measurements show the presence of moderate antiferromagnetic exchange interactions (ferrimagnetic) in all the cases mediated through the double phenoxido bridges that have been fitted with an anisotropic model including spin−orbit coupling in the central Co(II) ion.

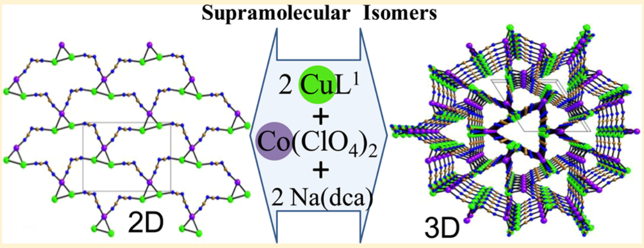

■ INTRODUCTION

Coordination polymers (CP) of first transition-metal ions is one the most developed areas by inorganic chemists or material scientists in the last few decades. These supramolecular architectures are readily self-assembled from the appropriate metal ions and organic linkers through coordination bonds. There are various factors such as coordination geometry of the metal atom, temperature, pH value, solvent systems, flexibility of the ligands, ligand-to-metal ratios, counterions, etc. that can potentially influence the construction of the frameworks of CPs.[1] Several methods have been used for the synthesis of CPs. Among them, Robson et al.[2] exemplified arguably the most attractive model, named the "node-and-spacer" approach for the synthesis of a large variety of CPs, and since then it has become a widely employed strategy to obtain CPs of various dimensionalities and network topologies.[2] Although, most of the reported CPs are constructed from a single metal center as a node, there are several reports where oligonuclear complexes have been used as nodes.[3] The presence of two or more metal ions confers a higher geometrical flexibility to the node. In the case of binuclear nodes, two metal ions or only one of them can be involved in the interaction with the spacers. When these two metal ions differ drastically in their chemical behavior (hard/soft character), then various types of coordination polymers can be obtained from the selective interaction of the metal ions with the spacers.[4] On the other hand, the use of trinuclear metal complexes as node is very rare. Recently we have found that heterometallic trinuclear clusters of salen-type Schiff base ligands can conveniently be used as nodes, and due to the conformational flexibility of such species, they have proved to be very useful for the construction of supramolecular isomers.[5]

In supramolecular chemistry, the spacer is a planned species, whose encoded information is read by the metal ions according to their coordinating modes. However, slight variation in the way it links the metal ion may result in structurally different CPs with a fixed chemical composition, commonly known as supramolecular isomers or, less frequently, in linkage isomers.[6] When the crystals contain different guest or solvent molecules, "supramolecular isomerism" is usually referred to as pseudopolymorphism.[7] Examples of pseudopolymorphs can be found very often, but supramolecular isomers are very rare; therefore, the design and synthesis of such isomers pose a challenge to the synthetic chemists. In this regard, the dicyanamide ($N(CN)_2^-$ = dca^-) spacer is potentially an excellent candidate to construct supramolecular isomers due to its conformational flexibility and

Received: September 17, 2013
Published: February 19, 2014

dx.doi.org/10.1021/ic4023536 | Inorg. Chem. 2014, 53, 2441−2449

versatile coordination modes.[8] In the common $\mu_{1,5}$ bidentate bridging mode, the V-shaped dca$^-$ can orient itself in different directions to coordinate the metal ions. Moreover, it possesses other coordination modes as $\mu_{1,3,5}$-dca$^-$,[9] $\mu_{1,1,3,5}$-dca$^-$,[10] and $\mu_{1,1,3,5,5}$-dca$^-$.[11] Considering the flexibility and versatile coordination modes of dca$^-$, formation of a large number of supramolecular isomers is expected. However, to date only seven supramolecular isomers with dca$^-$ have been reported;[5a,12] four of them (two isomeric pairs) possess three-dimensional (3D) structures where a single metal center, Zn^{2+} or Cu^{2+}, acts as node. The three remaining examples, recently reported by us using a trinuclear Cu_2Cd cluster, present structures varying from an hexanuclear cluster to a one-dimensional (1D) ladder and a 1D zigzag chain.[5a]

Herein, we report the synthesis, crystal structure, and magnetic properties of three novel Cu_2Co complexes: the discrete trinuclear complex $[(CuL^2)_2Co\{dca\}_2]\cdot H_2O$ (**1**), the two-dimensional (2D) polymer $[(CuL^1)_2Co\{dca\}_2]$ (**2a**), and the 3D polymer $[(CuL^1)_2Co\{dca\}_2]$ (**2b**); where H_2L^1 and H_2L^2 are the di-Schiff bases *N*,*N*′-bis(salicylidene)-1,3-propanediamine and *N*,*N*′-bis(*α*-methylsalicylidene)-1,3-propanediamine, respectively. Polymers **2a** and **2b** are rare supramolecular isomers and crystallize as a mixture of products, although they are clearly distinguishable for their distinctly different color and thus can be easily separated by hand. Furthermore, compounds **1**, **2a**, and **2b** are heterometallic $Cu^{II}{}_2Co^{II}$ clusters where ferri- or ferromagnetic exchange interactions are expected to occur, depending on the structural parameters of the bridges. Variable-temperature magnetic susceptibility measurement of the discrete trinuclear compound **1** and of both the supramolecular isomers **2a** and **2b** are presented. The magnetic properties are modeled using an anisotropic exchange model.

■ EXPERIMENTAL SECTION

Starting Materials. Salicylaldehyde, 2-hydroxyacetophenone, and 1,3-propanediamine were purchased from Lancaster and were of reagent grade. They were used as received, without further purification.

> ***Caution!*** *Perchlorate salts of metal complexes with organic ligands are potentially explosive. Only a small amount of material should be prepared, and it should be handled with care.*

Synthesis of the Schiff Base Ligands H_2L^1 and H_2L^2 and Their Metallo-Ligands $[CuL^1]$ and $[CuL^2]$. The two di-Schiff-base ligands H_2L^1 and H_2L^2 were prepared by standard methods:[13] 5 mmol of 1,3-propanediamine (0.42 mL) were mixed with 10 mmol of the required carbonyl compounds: salicylaldehyde (1.04 mL) or 2-hydroxyacetophenone (1.21 mL) in methanol (20 mL). The resulting solutions were refluxed for ca. 2 h and allowed to cool. The yellow-colored methanolic solutions were used directly for complex formation. To a methanolic solution (20 mL) of $Cu(ClO_4)_2\cdot 6H_2O$ (1.852 g, 5 mmol) was added a methanolic solution of H_2L^1 or H_2L^2 (5 mmol, 10 mL) to prepare the respective "metallo-ligands" $[CuL^1]$[13a] and $[CuL^2]$[13b] as reported earlier (Scheme 1).

Synthesis of the Complexes $[(CuL^2)_2Co\{dca\}_2]\cdot H_2O$ (1), $[(CuL^1)_2Co\{dca\}_2]_n$ (2a), and $[(CuL^1)_2Co\{dca\}_2]_n$ (2b). The metallo-ligand $[CuL^2]$ (0.744 g, 2 mmol) was dissolved in methanol (30 mL). To this solution a methanolic solution (10 mL) of cobalt perchlorate (0.365 g, 1 mmol) was added with continuous stirring. An aqueous solution (10 mL) of sodium dicyanamide (0.178 g, 2 mmol) was then added to this solution with stirring. The solution was allowed to stand in open atmosphere for slow evaporation of the solvent. The brown X-ray quality single crystals of complex **1** started to appear at the bottom of the vessel in a few days. After 4 d, the crystals were isolated, washed with Et_2O, and dried in a vacuum desiccator containing anhydrous $CaCl_2$. Complexes **2a** and **2b** were obtained as a mixture of products following a procedure similar to that of **1**, except that the metallo-ligand $[CuL^1]$ (0.688 g, 2 mmol) was used instead of $[CuL^2]$. The color of complex **2a** is greenish-brown, whereas complex **2b** is green. The crystals for X-ray analysis and other physicochemical studies (IR and UV–visible (UV/vis) spectroscopy, powder X-ray diffraction (XRD), and magnetic measurements) have been separated easily by naked eye detection.

Scheme 1. Ligands and Metallo-Ligands Used in This Work

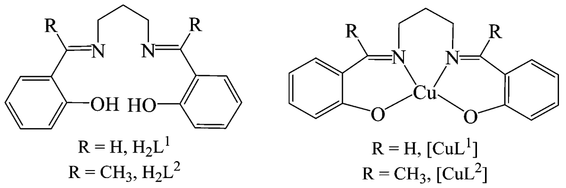

Complex 1. Yield: 0.724 g. (76%). Anal. Calcd for $C_{42}H_{42}CoCu_2N_{10}O_5$ (952.89): C 52.94, H 4.44, N 14.70. Found C 52.81, H 4.57, N 14.97%. UV/vis (MeCN): λ_{max} = 1120, 605, 327, 265, 216 nm. IR: ν(C=N); 1598 cm^{-1}, $\nu\{N(CN)_2\}$; 2270, 2225, and 2158 cm^{-1}.

Complex 2a. Yield: 0.302 g. (34%). Anal. Calcd for $C_{38}H_{32}CoCu_2N_{10}O_4$ (878.77): C 51.94, H 3.67, N 15.94. Found C 52.11, H 3.78, N 16.07%. UV/vis (MeCN): λ_{max} = 1102, 607, 337, 268, 237, 215 nm. IR: ν(C=N); 1619 cm^{-1}, $\nu\{N(CN)_2\}$; 2275, 2220, and 2156 cm^{-1}.

Complex 2b. Yield: 0.330 g. (38%). Anal. Calcd for $C_{38}H_{32}CoCu_2N_{10}O_4$ (878.77): C 51.94, H 3.67, N 15.94. Found C 51.71, H 3.87, N 15.98%. UV/vis (MeCN): λ_{max} = 1094, 610, 337, 269, 237, 216 nm. IR: ν(C=N); 1619 cm^{-1}, $\nu\{N(CN)_2\}$; 2273, 2226, and 2158 cm^{-1}.

Crystal Data Collection and Refinement. Suitable single crystals were mounted on a Bruker-AXS SMART APEX II diffractometer equipped with a graphite monochromator and Mo Kα (λ = 0.71073 Å) radiation. The crystals were positioned at 60 mm from the charge-coupled device (CCD). 360 frames were measured with a counting time of 10s. The structures were solved using Patterson method by using the SHELXS97 software. Subsequent difference Fourier synthesis and least-squares refinement revealed the positions of the remaining non-hydrogen atoms. Non-hydrogen atoms were refined with independent anisotropic displacement parameters. Hydrogen atoms were placed in idealized positions, and their displacement parameters were fixed to be 1.2 times larger than those of the attached non-hydrogen atom. Successful convergence was indicated by the maximum shift/error of 0.001 for the last cycle of the least-squares refinement. In **2b**, two carbon atoms (C10 and C11) were disordered over two positions (C10a, C10b and C11a, C11b). However, C9a and C9b, and also N2a and N2b, were identical but had to be included separately, as C9 had hydrogen atoms in different places because of the disorder between C10a and C10b, as N2 held in between C10 and C11. The disordered atoms were also refined with 50% occupancy. Absorption corrections were carried out using the SADABS program.[14] All calculations were carried out using SHELXS 97,[15] SHELXL 97,[16] PLATON 99,[17] ORTEP-32,[18] and WinGX

Table 1. Crystal Data and Structure Refinement for Complexes 1, 2a, and 2b

complex	1	2a	2b
mol. formula	$C_{42}H_{42}Cu_2CoN_{10}O_5$	$C_{38}H_{32}Cu_2CoN_{10}O_4$	$C_{38}H_{32}Cu_2CoN_{10}O_4$
formula wt.	952.89	878.77	878.77
space group	$C2/c$	$P2_1/c$	$P3_221$
crystal system	monoclinic	monoclinic	trigonal
a (Å)	23.2919(9)	16.314(5)	11.447(5)
b (Å)	10.4559(4)	10.792(5)	11.447(5)
c (Å)	17.3059(7)	21.913(5)	24.454(5)
α (deg)	90	90	90
β (deg)	97.357(2)	106.668(5)	90
γ (deg)	90	90	120
V (Å^3)	4179.9(3)	3696(2)	2775(3)
Z	4	4	3
d_{cal} (g cm^{-3})	1.514	1.579	1.578
μ (mm^{-1})	1.458	1.640	1.638
R_{int}	0.0530	0.0516	0.0772
no. of unique data	3624	6747	3798
data with I > 2σ(I)	2906	4843	3096
R1 on $I > 2\sigma(I)$	0.0392	0.0375	0.0446
wR2 on $I > 2\sigma(I)$	0.1016	0.0812	0.1026
GOF on F^2	1.077	1.023	1.035

Scheme 2. Synthetic Route to the Complexes 1, 2a, and 2b

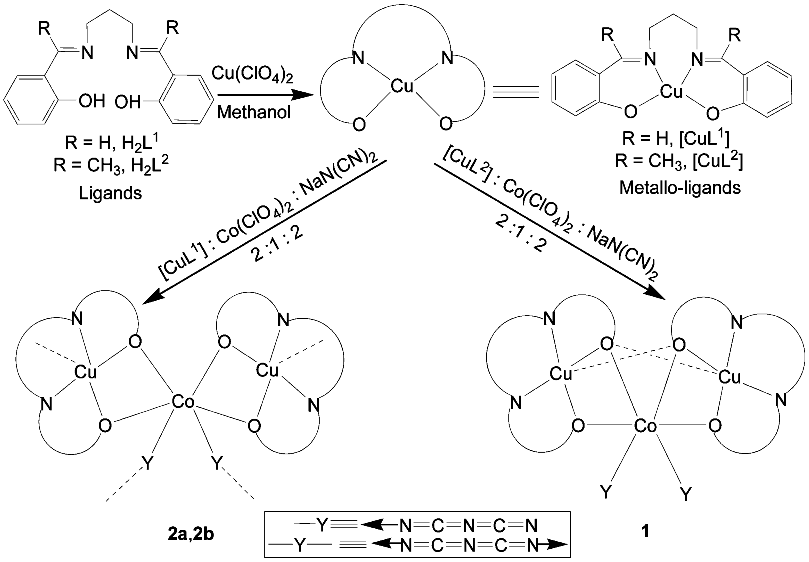

system Version 1.64.[19] Data collection and structure refinement parameters and crystallographic data for the three crystals are given in Table 1.

Physical Measurements. Elemental analyses (C, H, and N) were performed using a Perkin-Elmer 2400 series II CHN analyzer. IR spectra in KBr pellets (4500−500 cm^{-1}) were recorded using a Perkin-Elmer RXI FT-IR spectrophotometer. The electronic absorption spectra in acetonitrile solution (1400−200 nm) and in solid state (1400−250 nm) were recorded in a Hitachi U-3501 spectrophotometer. Powder XRD patterns are recorded on a Bruker D-8 Advance diffractometer operated at 40 kV voltage and 40 mA current and calibrated with a standard silicon sample, using Ni-filtered Cu Kα (α = 0.15406 nm) radiation. Experimental and simulated powder XRD plots are given in Supporting Information, Figures S5−S7 for compounds **1**, **2a**, and **2b**, respectively.

Variable-temperature susceptibility measurements were carried out in the temperature range of 2−300 K with an applied magnetic field of 0.1 T on polycrystalline samples of the three compounds (with masses of 11.02, 32.87, and 36.29 mg for compounds **1**, **2a**, and **2b**, respectively) with a Quantum Design MPMS-XL-5 SQUID magnetometer. The susceptibility data were corrected for the sample holders previously measured, using the same conditions and for the diamagnetic contributions of the salt as deduced by using Pascal's constant tables (χ_{dia} = −498.22 × 10^{-6}, −429.86 × 10^{-6}, and −477.3 × 10^{-6} emu mol^{-1} for **1**, **2a**, and **2b**, respectively).

RESULTS AND DISCUSSION

Synthesis, IR, and UV−vis Absorption Considerations. The di-Schiff base ligands (H_2L^1 and H_2L^2) and their Cu^{II} complexes ([CuL^1] and [CuL^2]) were synthesized using the reported methods.[13] These metallo-ligands react with Co-

$(ClO_4)_2{\cdot}6H_2O$ and sodium dicyanamide in MeOH−H_2O medium (4:1, v/v) to form a trinuclear complex and two polymeric isomers. Complex $[(CuL^2)_2Co\{dca\}_2]{\cdot}H_2O$ (**1**) is a discrete trinuclear species where two dicyanamide anions coordinate to the central Co(II) ion as terminal cis-monodentate ligands. On the other hand, when the metallo-ligand is $[CuL^1]$, the dca^- ligands connected to the central Co(II) ion act as bridges to connect each Co(II) to one of the axial positions of the copper atom of two neighboring trinuclear units in two different ways to produce a 2D polymer $[(CuL^1)_2Co\{dca\}_2]_n$ (**2a**) or a 3D polymer $[(CuL^1)_2Co\{dca\}_2]_n$ (**2b**) (Scheme 2). Note that, in the three complexes, two metallo-ligands coordinate to a central Co(II) ion along with two cis coordinated dicyanamide ions, forming identical Cu_2Co trinuclear units (except for the terminal L^2 and L^1 ligands). Albeit, the overall structures of the three compounds are quite different (see below).

Besides elemental analysis, all complexes were initially characterized by IR spectra. The metallo-ligands ($[CuL^1]$ and $[CuL^2]$) are neutral and hence do not have any counteranion, whereas complexes **1**, **2a**, and **2b** contain two coordinated dca^- anions to balance the charge of the central Co(II) ion. The complexes exhibit ν_{C-N} bands at 2270, 2225, and 2158 cm^{-1} for **1**, 2275, 2220, and 2156 cm^{-1} for **2a**, and 2273, 2226, and 2158 cm^{-1} for **2b**, which are attributed to $\nu_{sym} + \nu_{asym}$ (CN), ν_{asym} (CN), and ν_{sym} (CN) modes of the bridging dca^- ligand, respectively. The IR spectra also show strong and sharp bands due to the azomethine $\nu_{C=N}$ group of the Schiff base, appearing at 1598, 1619, and 1619 cm^{-1} for complexes **1**, **2a**, and **2b**, respectively. The $\nu_{C=N}$ bands of the free ligands H_2L^1 and H_2L^2 appear at 1628 and 1608 cm^{-1}, respectively. The lower value of the band position indicates the coordination of the azomethine group to the metal ion. In the IR spectra of complex **1**, a broad band near 3447 cm^{-1} is attributed to the O−H stretching of the water molecule.

The electronic spectra of the three complexes were recorded in acetonitrile solutions (Supporting Information, Figure S1). The spectrum of complex **1** displays a single absorption band at 1120 nm and a shoulder near 605 nm (Supporting Information, Figure S1a). The positions of these bands are consistent with d−d transitions in cobalt(II) ions with octahedral geometry. The shoulder of the band at ca. 600 nm may be attributed to octahedralCo(II) ($^4A_{2g}(F) \leftarrow {}^4T_{1g}(F)$) or to square-based Cu(II) ($^2T_{2g} \leftarrow {}^2E_g$). The charge transfer (CT) bands are observed at 327, 265, and 216 nm (Supporting Information, Figure S1b). The spectra of complexes **2a** and **2b** are very similar to each other. They show two separated d−d transition bands at 1102 and 607 for **2a** and at 1094 and 610 nm for **2b**. Four distinct CT bands in the spectra of both complexes appear at 337, 268, 237, 215 nm in **2a** and 337, 269, 237, 216 nm in **2b**. The UV/vis spectra of the two isomers **2a** and **2b** are also measured in solid-state diffused reflectance spectra (Supporting Information, Figure S2). The compounds exhibit two broad absorption bands in the visible region at the 530−660 and at the 1250−1350 nm regions. Besides these broad bands, both products show two separated sharp single absorption maxima near 358, 283 nm for **2a** and 367, 289 nm for **2b**, attributed to ligand-to-metal CT transitions (near 360 nm) and $\pi-\pi^*$ transition within the ligand (near 280 nm).

Description of Structures of the Complexes.

$[(CuL^2)_2Co\{dca\}_2]{\cdot}H_2O$ (1). Compound **1** consists of discrete trinuclear units of formula $[(CuL^2)_2Co\{dca\}_2]$ with a crystallographic 2-fold axis passing through the cobalt atom. The trinuclear complex contains a central cobalt ion coordinated to two *cis*-terminal dca^- ligands and to four phenoxido oxygen atoms from two terminal $[CuL^2]$ chelating units (Figure 1).

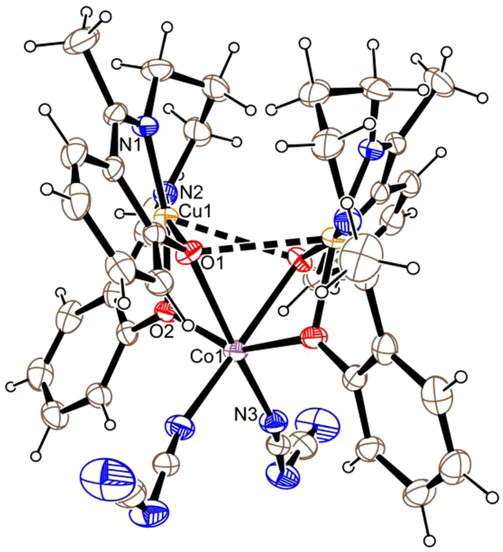

Figure 1. ORTEP view of complex **1** with ellipsoids at 30% probability. Dashed lines represent the two equivalent long semi-coordinate Cu−O bonds (Cu1−O1 = 2.719(2) Å).

Table 2. Bond Distances (Å) and Angles (deg) around the Metal in Centers Complex 1

atoms	distance	atoms	distance
Cu1−O1	1.908(3)	Cu1−O1*	2.718(2)
Cu1−O2	1.923(2)	Co1−O1	2.273(2)
Cu1−N1	1.945(3)	Co1−O2	2.005(2)
Cu1−N2	1.970(3)	Co1−N3	2.061(3)
atoms	angle	atoms	angle
O1−Cu1−O2	83.48(10)	O1−Co1−O2	72.88(9)
O1−Cu1−N1	90.43(12)	O1−Co1−N3	166.02(11)
O1−Cu1−N2	165.90 (11)	O1−Co1−O1*	72.23(8)
O1−Cu1−O1*	68.22(8)	O1−Co1−O2*	82.80(9)
O2−Cu1−N1	165.80(12)	O1−Co1−N3*	98.73(10)
O2−Cu1−N2	89.82(12)	O2−Co1−N3	95.77(11)
O1*−Cu1−O2	73.10(8)	O2−Co1−O2*	149.89(9)
N1−Cu1−N2	98.74(14)	O2−Co1−N3*	105.09(11)
O1*−Cu1−N1	116.47(11)	N3−Co1−N3*	92.02(13)
O1*−Cu1−N2	97.97(10)	symmetry element * = 2 − *x*, *y*, 1/2 − z	

The bond distances and angles are given in Table 2. The Cu(II) ions present a pentacoordinated square pyramidal geometry, where the basal plane is formed by the two imine N atoms N(1) and N(2) and the two phenoxido O atoms O(1) and O(2) of the chelating Schiff base. The two $[CuL^2]$ units in the molecule are connected through the semicoordination of one of the phenoxido oxygen atoms of one unit, O(1), to the axial position of the copper atom (Cu1*) of the other $[CuL^2]$ unit, with a Cu(1)*−O(1) distance of 2.718(2) Å (symmetry element * = 2 − *x*, *y*, 1/2 − *z*). This semicoordination leads to a Cu···Cu distance of 3.695(1) Å. The root-mean-square (r.m.s.) deviation of the four basal atoms from the mean plane passing through them is 0.199 Å. The metal atom is 0.004(1) Å from this plane toward the axially coordinated oxygen atom. The Addison parameter[20] of the Cu atom is 0.001, indicating an almost perfect square pyramidal geometry.

The central Co(1) atom lies on a 2-fold axis and is bonded to two N atoms from two cis-coordinated terminal dca$^-$ ligands and to four oxygen atoms from two bidentate chelated [CuL^2] units in a highly distorted octahedral arrangement. The six bond distances around Co(II) ion lie in the range of 2.019(2)–2.272(2) Å (Table 2). The cis N–Co–N angle [92.04(13)°] formed by the two dca$^-$ groups is close to the ideal value of 90°, but those involving the two oxygen atoms from the chelated [CuL^2] metallo-ligand [72.87(9)°] are far from the ideal values. The three trans angles [between 149.88(9) and 166.03(11)°] are also considerably smaller than the ideal ones.

[(CuL^1)$_2$Co{dca}$_2$]$_n$ ***(2a).*** Compound **2a** presents a 2D polymeric structure formed by trinuclear units [(CuL^1)$_2$Co{dca}$_2$] connected by bridging dca$^-$ anions. These trinuclear units contain two terminal [CuL^1] entities, one central Co(II) atom, and two dca$^-$anions coordinated to the Co(II) ion (Figure 2). The bond distances and angles are given in Table 3.

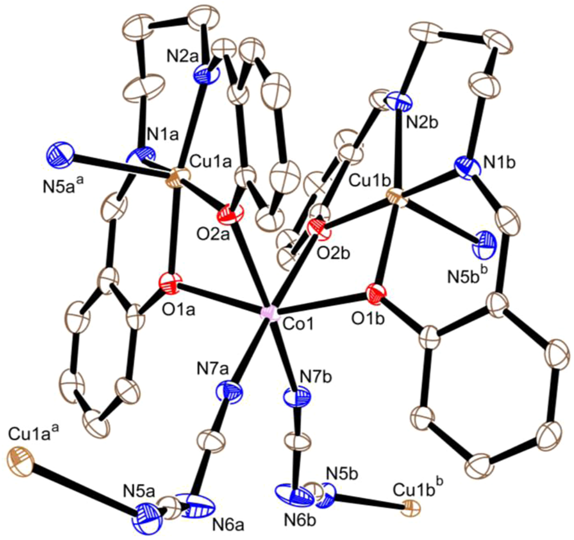

Figure 2. ORTEP view of complex **2a** with ellipsoids at 30% probability. Hydrogen atoms are omitted for clarity. Symmetry element ^{a} = 1 − *x*, 1/2 + *y*, 1/2 − *z* and ^{b} = −*x*, *y* + 1/2, 1/2 − *z*.

Both copper atoms Cu(1) and Cu(2) present a square pyramidal geometry, where the basal plane is formed by the two imine N atoms [N(1) and N(2) for Cu(1); N(3) and N(4) for Cu(2)] and the two phenoxido O atoms [O(1) and O(2) for Cu(1); O(3) and O(4) for Cu(2)] of the corresponding L^2 ligand. The axial positions are occupied by the nitrogen atoms [N(7) and N(10) for Cu(1) and Cu(2), respectively] of two different $\mu_{1,5}$-dca$^-$ anions connecting the Cu(II) ions of one trimer with two other Cu$_2$Co units (Figure 2). The r.m.s. deviations of the four basal atoms from the mean plane passing through them are 0.017 and 0.012 Å for Cu(1) and Cu(2), respectively. The metal atoms Cu(1) and Cu(2) are located 0.151(1) and 0.141(1) Å away from this plane toward the axially coordinated nitrogen atom of the dca$^-$ coligands. The Addison parameter[20] of the Cu(1) and Cu(2) atoms are 0.028 and 0.007, indicating, as in **1**, an almost perfect square pyramidal geometry.

The central Co(1) atom is bonded to four phenoxido oxygen atoms, two from each of the two [CuL^1] units and two cis-coordinated nitrogen atoms from two different dca$^-$ coligands, giving rise to a distorted octahedral geometry. The O–Co–O cis angles subtended at the metal centers by the chelating [CuL^1] units are 74.4(1)° and 72.1(1)°, whereas the two cis-coordinated dca$^-$ ligands present a N–Co–N bond angle of 90.3(1)° (Table 3). On the other hand, the three trans angles, in the range of 155.1(1)–171.4(1)°, indicate an important distortion of the central cobalt atom from the ideal octahedral geometry, although smaller than in **1**. The Cu(1)···Co(1), Cu(2)···Co(1), and Cu(1)···Cu(2) distances are 3.089(2), 3.032(2), and 4.020(2) Å, respectively.

[(CuL^1)$_2$Co{dca}$_2$]$_n$ ***(2b).*** Compound **2b** has the same molecular formula [(CuL^1)$_2$Co{dca}$_2$]$_n$ as **2a**, but the polymeric structure is 3D instead of 2D (see below). The asymmetric unit of complex **2b** contains one [CuL^1] unit, one dca$^-$ anion, and one Co(II) atom sitting on a 2-fold axis (Figure 3). The bond distances and angles are given in Table 3. As in **2a**, the terminal copper atom in **2b** has a square pyramidal geometry, with the basal plane formed by the two imine N atoms N(1) and N(2) and the two phenoxido O atoms O(1) and O(2) of the Schiff base. The axial position is occupied by a nitrogen atom (N7) of a $\mu_{1,5}$-dca$^-$ ligand. The r.m.s. deviations of the four basal atoms from the mean plane passing through them is 0.038 Å. The metal atom is located 0.145(1) Å away from this plane toward the axially coordinated nitrogen atom of the dca$^-$ coligand. The Addison parameter[20] of Cu(1) is 0.057, indicating a small distortion from the ideal square pyramidal geometry.

The central Co atom sits on a 2-fold axis and is coordinated by four phenoxido oxygen atoms from two [CuL^1] units and two nitrogen atoms from two dca$^-$ ligands. The bond lengths around Co(1) are in the range of 2.056(3)–2.161(3) Å. The chelating [CuL^1] unit and the two cis-coordinated dca$^-$ ligands form cis angles of 71.6(1)° and 90.2(2)°, respectively (Table 3). On the other hand, the three trans angles lie in the range of 152.1(1)–171.2(2)°, indicating a very similar distortion of the coordination environment around the cobalt atom in **2a** and **2b**. The Cu(1)···Co(1) and Cu(1)···Cu(1)′ distances are 3.069(2) and 4.009(2) Å (symmetry element ′ = −*x*, −*x* + *y*, −*z* + 2/3).

Origin of the Differences in the Dimensionality of the Two Coordination Polymers ***2a*** *and* ***2b.*** Although, as already indicated, both complexes **2a** and **2b** contain the same molecular composition [(CuL^1)$_2$Co{dca}$_2$], that is, triangular Cu$_2$Co nodes connected by four $\mu_{1,5}$-dca bridges with four neighboring Cu$_2$Co nodes (forming uninodal 4-connected nets), their polymeric structures are different: compound **2a** presents a 2D structure, whereas **2b** is a 3D network. Since these two compounds have identical chemical compositions but differ only in their spatial superstructures, they are rare examples of supramolecular isomers. Moreover, compounds **2a** and **2b** are even rarer examples of supramolecular isomers that are clearly distinguishable by naked eye since complex **2a** is greenish-brown, whereas **2b** is green.

The Cu–Co–Cu angles inside the trimeric angular Cu$_2$Co nodes are also very similar (82.10(2)° and 81.55(3)° for **2a** and **2b**, respectively), as is the geometry of the bridging $\mu_{1,5}$-dca$^-$ anions (V-shaped with N–N–N vertex angles of 124.0(3)° and 123.2(3)° in **2a** and 122.8(6) in **2b**). Furthermore, the two $\mu_{1,5}$-dca$^-$ anions are cis-coordinated to the central cobalt atom (Figures 2 and 3). The question is then why are the compounds different? In fact, the only difference between two structures is the spatial disposition of the bridges: in **2a** the

Table 3. Comparing the Bond Distances (Å) and Angles (deg) around the Metal Centers in Both Isomers **2a** and **2b**

2a			2b	
	unit A	unit B		
atoms	distances	distances	atoms	distances
Cu1−O1	1.956(2)	1.951(2)	Cu1−O1	1.925(3)
Cu1−O2	1.950(2)	1.949(2)	Cu1−O2	1.939(5)
Cu1−N1	1.977(7)	1.976(3)	Cu1−N1	1.971(7)
Cu1−N2	1.966(6)	1.978(3)	Cu1−N2A	1.966(6)
Cu1−N5^a	2.379(4)	2.296(4)	Cu1−N5″^{b}	2.456(6)
Co1−O1	2.094(2)	2.056(2)	Co1−O1	2.055(3)
Co1−O2	2.124(3)	2.172(3)	Co1−O2	2.159(3)
Co1−N7	2.080(3)	2.060(3)	Co1−N7	2.075(6)
Co1−Cu1	3.032(2)	3.089(2)	Co1−Cu1	3.070(2)
atoms	angle	angle	atoms	angle
O1−Cu1−O2	78.9(1)	82.0(1)	O1−Cu1−O2	79.5(1)
O1−Cu1−N1	92.0(1)	90.0(1)	O1−Cu1−N1	90.9 (2)
O1−Cu1−N2	167.3(1)	169.4(1)	O1−Cu1−N2A	169.1(2)
O1−Cu1−N5^a	99.3(1)	94.2(1)	O1−Cu1−N5″^{b}	94.0(2)
O2−Cu1−N1	167.7(1)	167.7(1)	O2−Cu1−N1	165.9(2)
O2−Cu1−N2	90.3(1)	90.2(1)	O2−Cu1−N2A	92.2(3)
O2−Cu1−N5^a	94.3(1)	92.5(1)	O2−Cu1−N5″^{b}	102.9(3)
N1−Cu1−N2	97.6(1)	96.5(1)	N1−Cu1−N2A	95.9(3)
N1−Cu1−N5^a	95.4(1)	97.4(1)	N1−Cu1−N5″^{b}	87.9(3)
N2−Cu1−N5^a	88.2(1)	93.3(1)	N2A−Cu1−N5″^{b}	94.8(3)
O1−Co1−O2	72.1(1)	74.4(1)	O1−Co1−O2	71.7(1)
O1−Co1−N7	99.0(1)	98.8(1)	O1−Co1−N7	99.7(2)
O2−Co1−N7	96.1(1)	95.2(1)	O2−Co1−N7	94.3(2)
O1A−Co1−O1B	155.1(1)		O1−Co1−O1′^{b}	152.2(2)
O1A−Co1−O2B	86.7(1)		O1−Co1−O2′^{b}	87.3(1)
O1A−Co1−O2B	79.5(1)		O2−Co1−O2′^{b}	82.5(2)
O2A−Co1−N7B	169.7(1)		O2′−Co1−N7^b	171.1(2)
O1A−Co1−N7B	98.9(1)		O2−Co1−N7′^{b}	99.9(2)
N7A−Co1−N7B	90.3(1)		N7−Co1−N7′^{b}	90.1(2)
Co1−O1−Cu1	96.9(1)	100.9(1)	Co1−O1−Cu1	100.9(1)
Co1−O2−Cu1	96.1(1)	97.0(1)	Co1−O2−Cu1	96.9(2)
O1B−Co1−N7A		98.3(1)		
O1B−Co1−O2A		88.4(1)		
O2B−Co1−N7A		171.4(1)		

^{a}Symmetry operation = $1 - x$, $1/2 + y$, $1/2 - z$ for A unit and $-x$, $1/2 + y$, $1/2 - z$ for B unit of compound **2a**. ^{b}Symmetry operation ′ = $-x$, $-x + y$, $2/3 - z$ and ″ = $x - y$, $1 - y$, $1/3 - z$ for **2b**.

four $\mu_{1,5}$-dca$^-$ anions connect each Cu$_2$Co unit with four similar Cu$_2$Co units in the same plane (Figure 4a), giving rise to a 2D square lattice (Figure 4b), whereas in **2b** these four Cu$_2$Co nodes are distributed in two different planes with a distorted tetrahedral orientation (Figure 4c), giving rise to a 3D structure formed by interconnected triangular layers (Figure 4d).

Magnetic Properties. The three compounds present, as expected, very similar magnetic properties (Figure 5). The product of the molar magnetic susceptibility times the temperature ($\chi_m T$) per Cu$_2$Co trimer shows room temperature values of ca. 3.90, 3.88, and 3.80 emu K mol^{-1} for compounds **1**, **2a**, and **2b**, respectively. These values are within the normal range expected for two noninteracting Cu(II) ions and a Co(II) ion. Thus, if we subtract the expected contribution for two Cu(II) ions (ca. 0.80 emu K mol^{-1}), we obtain values of ca. 3.10, 3.08, and 3.00 emu K mol^{-1} for the Co(II) contribution of compounds **1**, **2a**, and **2b**, respectively (within the normal range of 2.8−3.4 emu K mol^{-1} observed in isolated Co(II) complexes).[21] These values are above the expected ones for an $S = 3/2$ spin ground state (1.875 emu K mol^{-1}) since high spin Co(II) octahedral complexes present an orbital contribution arising from the $^4T_1$ ground state. When the temperature is decreased, $\chi_m T$ shows a continuous decrease to reach a smooth plateau of ca. 0.3 emu K mol^{-1} at low temperature (or a small bump in compound **2b**, attributed to the presence of a small fraction of a ferromagnetic impurity). The decrease in the observed $\chi_m T$ may be due to two possible reasons: on one hand, it may be a consequence of the first-order spin−orbit coupling present in isolated Co(II) complexes and, on the other hand, it may be due to the presence of an antiferromagnetic coupling between the central Co(II) ion and the terminal Cu(II) ones. Since the spin−orbit coupling in isolated Co(II) complexes usually leads to $\chi_m T$ values at low temperature in the range of 1.0−2.0 emu K mol^{-1}, well above the observed value of ca. 0.3 emu K mol^{-1}, we can conclude that the three compounds present an antiferromagnetic coupling between the central Co(II) ion and the terminal Cu(II) ones.

A confirmation of the ferrimagnetic coupling is provided by the thermal variation of the molar susceptibility χ_m that shows rounded maxima at ca. 50, 65, and 60 K for compounds **1**, **2a**, and **2b**, respectively, which are slightly masked by the intense

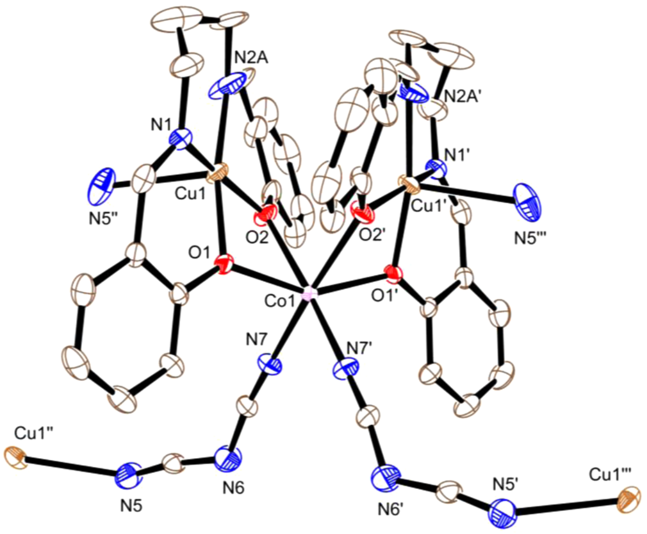

Figure 3. ORTEP view of complex **2b**, with ellipsoids at 30% probability. Hydrogen atoms are omitted for clarity. Symmetry element ′ = −*x*, −*x* + *y*, −*z* + 2/3; ″ = *x* − *y*, 1 − *y*, −*z* + 1/3; ‴ = −*x* + *y*, −*x*, *z* + 1/3.

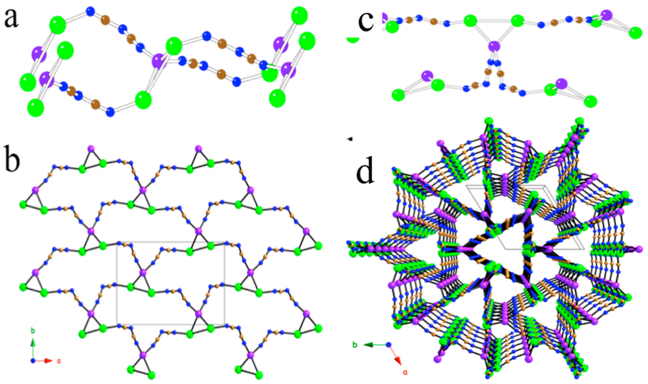

Figure 4. (a) Planar connectivity of the Cu_2Co nodes in compound **2a** and (b) the resulting 2D square lattice. (c) Distorted tetrahedral connectivity of the Cu_2Co nodes in compound **2b** and (d) the resulting 3D structure. Color code: Cu = green, Co = purple, N = blue, C = brown.

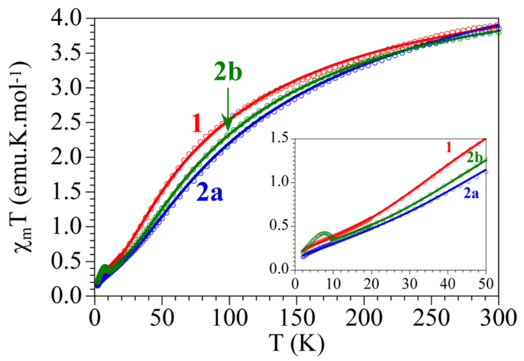

Figure 5. Thermal variation of the $\chi_m T$ product for the trinuclear $CoCu_2$ compounds **1**, **2a**, and **2b**. Inset shows the low-temperature region. Solid lines are the best fits to the anisotropic model (see text).

paramagnetic contribution of the *S* = 1/2 ground state at low temperatures (Curie tail) (not shown). This contribution of the *S* = 1/2 ground state is clearly seen in the isothermal magnetization at low temperatures that show saturation values close to 1 μ_B, the expected value for a *S* = 1/2 spin ground state with *g* = 2 (see Supporting Information, Figures S3 and S4).

Since the three compounds show a symmetric (**1** and **2b**) or nearly symmetric (in **2a**) trimer structure with a central Co(II) ion connected to two terminal Cu(II) ions through a double phenoxido bridge, we have used a model that considers a ground state of $^4T_1$ for the octahedral Co(II) ion with a *S* = 3/2 spin state with a fictitious angular momentum *L* = 1. The Hamiltonian for this triangular system contains three different terms: (i) an isotropic exchange interaction between Cu(II) and Co(II) real spins, based on the Lines model,[22] (ii) a spin−orbit interaction term in the Co(II) ion, and (iii) a term taking into account the effect of axial distortions:[23]

$$\hat{H} = -2J(S_{Cu1}S_{Co} + S_{Cu2}S_{Co}) + Ak\lambda S_{Co}L + D(L_z^2 + L(L + 1))$$

In this Hamiltonian *k* is the orbital reduction factor and *λ* is the spin−orbit coupling constant. The *A* factor, defined in the context of *T* and *P* term isomorphism, permits differentiation between the matrix elements of the orbital angular momentum operator calculated with the use of the *P* term basis from those calculated with the wave functions of the $^4T_1$ term.[24]

The Zeeman interaction is assumed to be isotropic and can be presented as:

$$\hat{H} = \beta(g_e S_{Co} + AkL)H + \beta g_{Cu}(S_{Co1} + S_{Co2})H$$

where the first term describes the interaction of an octahedral Co(II) ion with an external magnetic field including both spin and orbital Zeeman contributions (g_e is the electronic *g* factor) and the second term only considers the spin Zeeman contribution of the Cu(II) ions.

Since there is no analytical expression for fitting the magnetic properties with this anisotropic Hamiltoniam, the thermal variation of the molar magnetic susceptibility χ_m for the trinuclear Cu_2Co unit was simulated using an exact diagonalization process.[25] A very satisfactory fit of the $\chi_m T$ product is obtained for the three compounds with the parameters displayed in Table 4 (solid lines in Figure 5).

The spin−orbit coupling parameters are close to those observed for the free Co(II) ion (−160 cm^{-1}). The negative value of parameter Δ means that the doublet $^4E_2$ state is the fundamental and lies below the $^4A_2$ state by 550−770 cm^{-1}, a value which is reasonable for octahedral Co(II) ions.

The antiferromagnetic coupling observed in the three compounds can be explained from their structures. They all present double phenoxido bridges connecting the central Co(II) ion with the two terminal Cu(II) ones. It is well-known that the magnetic coupling through this kind of double alkoxido bridges is mainly controlled by the M−O−M bond angle and the dihedral angle within the M_2O_2 entity.[26] These correlations show that for M = Cu(II) the coupling is antiferromagnetic and increases (in absolute value) as the M−O−M angle increases. As expected, the coupling also increases (in absolute value) as the dihedral angle in the M_2O_2 unit decreases, becoming maximum when the M_2O_2 unit is planar.

In compounds **1**, **2a**, and **2b** the Cu−O−Co bond angles are 100.44(11)° and 92.07(10)° (in **1**), 100.84(9)°, 96.97(9)°, 96.12(9)°, and 96.90(9)° (in **2a**), and 100.91(14)° and 96.79(15)° (in **2b**) (Table 4). Although the above-mentioned correlations have been established for homometallic systems, we can conclude that for the angles present in compounds **1**,

Table 4. Magnetic and Structural Parameters of the Cu_2Co Complexes **1**, **2a**, and **2b**

parameter	1	2a	2b
$2J$ (cm^{-1})	−37.2	−51.6	−47.2
λ (cm^{-1})	−163.0	−160.0	−180.0
Δ (cm^{-1})	−758.9	−551.6	−769.3
Ak	−1.48	−1.41	−1.50
g_{Cu}	2.11	2.00	2.12
Tip (emu mol^{-1})	1.1×10^{-3}	2.6×10^{-3}	5.9×10^{-3}
R^a	1.5×10^{-3}	7.8×10^{-4}	6.7×10^{-3}
Cu−O−Co (deg)	100.47(10)	100.84(9)	100.91(14)
	92.06(9)	96.97(9)	96.79(15)
		96.12(9)	
		96.90(9)	
Cu−O (Å)	1.908(2)	1.951(2)	1.938(4)
	1.922(2)	1.948(2)	1.923(3)
		1.949(2)	
		1.956(2)	
Co−O (Å)	2.005(2)	2.056(2)	2.162(3)
	2.273(2)	2.172(2)	2.056(3)
		2.124(2)	
		2.094(2)	

[a] R is the error of the fitting process.

2a, and **2b** the Cu−Co coupling is expected to be antiferromagnetic and moderate, in agreement with the experimental results. Furthermore, since the average Cu−O−Co bond angles are significantly larger in compounds **2a** and **2b** (97.71° and 98.85°) than in **1** (96.26°), compounds **2a** and **2b** are expected to show a larger antiferromagnetic coupling, in agreement with the observed J values (Table 4). If we compare compounds **2a** and **2b**, we can see that both compounds present similar coupling constants. This is probably due to the fact that, although in **2b** the Cu−Co−Cu bond angles are larger (and, therefore, **2b** should present a stronger coupling), the CuO_2Co entity is significantly more planar in compound **2a** (18.3°) than in compound **2b** (25.2°), resulting in a decrease of the coupling constant in complex **2b**.

The antiferromagnetic interaction observed in compounds **1**, **2a**, and **2b** are of the same order as those of the only three reported Cu_2Co trimers with similar double oxido bridges. Albeit, we cannot establish any comparison since in two of these three complexes the model used to fit the magnetic properties was an isotropic one, only valid at high temperatures,[27] the third complex presents some important geometrical differences (the central Co(II) presents an elongated 4 + 2 coordination geometry), and the anisotropic model included a large zero-field splitting in the Co(II) ion ($|D| = 56$ cm^{-1}).[28]

■ CONCLUSIONS

Here we have shown that the reaction of two different metalloligands, [CuL^1] and [CuL^2], containing di-Schiff base ligands with cobalt(II) and dicyanamide anions, gives rise to three different compounds containing similar Cu_2Co trinuclear units where double phenoxido bridges connect the central Co(II) ion with the terminal Cu(II) ones. The most surprising result is the simultaneous crystallization of two different isomers, **2a** and **2b**, presenting the same Cu_2Co units and dca^- bridges with the same connectivity differing only in the spatial distribution of the bridges that leads to a 2D square lattice in **2a** and a triangular 3D lattice in **2b**. Furthermore, although **2a** and **2b** are almost identical, they present different colors, allowing an easy separation. From the magnetic point of view, as expected, the three compounds present very similar properties with a moderate antiferromagnetic Co−Cu exchange interaction that can be well-modeled with an anisotropic exchange model including a spin−orbit coupling in the central Co(II) ion.

■ ASSOCIATED CONTENT

Ⓢ Supporting Information

UV−vis spectra of the three complexes in acetonitrile solution (Figure S1) and both isomers (**2a** and **2b**) in solid phase (Figure S2). Isothermal magnetizations at 2 K for the three complexes (Figures S3 and S4). Experimental and simulated powder X-ray data of compounds **1**, **2a**, and **2b** (Figures S5−S7). Crystallographic data of all the complexes are given in CIF format. This material is available free of charge via the Internet at http://pubs.acs.org.

■ AUTHOR INFORMATION

Corresponding Author

*E-mail: ghosh_59@yahoo.com (A.G.).

Notes

The authors declare no competing financial interest.

■ ACKNOWLEDGMENTS

We thank CSIR, India for awarding a senior research fellowship [Sanction No. 09/028(0732)/2008−EMR−I] to S.B. Crystallography was performed at the DST−FIST, India-funded Single Crystal Diffractometer Facility at the Department of Chemistry, University of Calcutta. We thank the Spanish MINECO (Project CTQ2011-26507) and the Generalidad Valenciana (Prometeo and ISIC-nano Projects) for financial support. We are thankful to Prof. Michael G. B. Drew, School of Chemistry, The University of Reading, U.K., for helpful suggestions on crystallographic part of the isomer **2b**. The authors also thank the Department of Science and Technology (DST), New Delhi, India, for financial support (SR/S1/IC/0034/2012).

■ REFERENCES

(1) (a) Zheng, B.; Dong, H.; Bai, J.-F.; Li, Y.-Z.; Li, S.-H.; Scheer, M. *J. Am. Chem. Soc.* **2008**, *130*, 7778−7779. (b) Long, L.-S. *CrystEngComm* **2010**, *12*, 1354−1365. (c) Li, C.-P.; Du, M. *Chem. Commun.* **2011**, *47*, 5958−5972. (d) Han, Y.; Zhang, Z.-H. *Cryst. Growth Des.* **2011**, *11*, 3448−3455. (e) Kar, P.; Ida, Y.; Ishida, T.; Ghosh, A. *CrystEngComm* **2013**, *15*, 400−410. (f) Eddaoudi, M.; Moler, D. B.; Li, H.; Chen, B.; Reineke, T. M.; O'keeffe, M.; Yaghi, O. M. *Acc. Chem. Res.* **2001**, *34*, 319−330. (g) Lu, J.; Paliwala, T.; Lim, S. C.; Yu, C.; Niu, T.; Jacobson, A. J. *Inorg. Chem.* **1997**, *36*, 923−929.

(2) (a) Hoskins, B. F.; Robson, R. *J. Am. Chem. Soc.* **1990**, *112*, 1546−1554. (b) Gable, R. W.; Hoskins, B. F.; Robson, R. *J. Chem. Soc., Chem. Commun.* **1990**, 1677−1678.

(3) (a) Andruh, M. *Chem. Commun.* **2007**, 2565−2577. (b) Branzea, D. G.; Madalan, A. M.; Ciattini, S.; Avarvari, N.; Caneschi, A.; Andruh, M. *New J. Chem.* **2010**, *34*, 2479−2490. (c) Mousavi, M.; Béreau, V.; Costes, J.-P.; Duhayon, C.; Sutter, J.-P. *CrystEngComm* **2011**, *13*, 5908−5914. (d) Gheorghe, R.; Andruh, M.; Costes, J.-P.; Donnadieu, B. *Chem. Commun.* **2003**, 2778−2779.

(4) (a) Andruh, M. *Chem. Commun.* **2011**, *47*, 3025−3042. (b) Gheorghe, R.; Cucos, P.; Andruh, M.; Costes, J.-P.; Donnadieu, B.; Shova, S. *Chem.—Eur. J.* **2006**, *12*, 187−203.

(5) (a) Das, L. K.; Ghosh, A. *CrystEngComm* **2013**, *15*, 9444−9456. (b) Ghosh, S.; Mukherjee, S.; Seth, P.; Mukherjee, P. S.; Ghosh, A. *Dalton Trans.* **2013**, *42*, 13554−13564.

(6) Benmansour, S.; Setifi, F.; Triki, S.; Gómez-García, C. J. *Inorg. Chem.* **2012**, *51*, 2359−2365.

(7) (a) Schröder, M.; Champness, N. R. In *Encyclopedia of Supramolecular Chemistry;* Atwood, J. L.; Steed, P., Eds.; Marcel Dekker, Inc.: New York, 2004; pp 1420–1426. (b) Moulton, B.; Zaworotko, M. J. *Chem. Rev.* **2001**, *101*, 1629–1658. (c) Hennigar, T. L.; MacQuarrie, D. C.; Loiser, P.; Rogers, R. D.; Zaworotko, M. J. *Angew. Chem., Int. Ed.* **1997**, *36*, 972–973. (d) Masaoka, S.; Tanaka, D.; Nakanishi, Y.; Kitagawa, S. *Angew. Chem., Int. Ed.* **2004**, *43*, 2530–2534. (e) Abourahma, H.; Moulton, B.; Kravtsov, V.; Zaworotko, M. J. *J. Am. Chem. Soc.* **2002**, *124*, 9990–9991. (f) Huang, X.-C.; Zhang, J.-P.; Chen, X.-M. *J. Am. Chem. Soc.* **2004**, *126*, 13218. (g) Moulton, B.; Zaworotko, M. J. *Chem. Rev.* **2001**, *101*, 1629–1658. (h) Zhang, J.-P.; Huang, X.-C.; Chen, X.-M. *Chem. Soc. Rev.* **2009**, *38*, 2385–2396. (i) Benmansour, S.; Marchivie, M.; Triki, S.; Gómez-García, C. J. *Crystals* **2012**, *2*, 306–326.

(8) (a) Potocnák, I.; Dunaj-Jurco, M.; Miklos, D.; Kabesová, M.; Jäger, L. *Acta Crystallogr., Sect. C: Cryst. Struct. Commun.* **1995**, *51*, 600–602. (b) Dasna, I.; Golhen, S.; Ouahab, L.; Peña, O.; Daro, N.; Sutter, J. P. *C. R. Acad. Sci., Ser. IIc: Chim.* **2001**, *4*, 125–133. (c) Zheng, X.-D.; Jiang, L.; Feng, X.-L.; Lu, T.-B. *Dalton Trans.* **2009**, 6802–6808.

(9) Batten, S. R.; Robson, R.; Jensen, P.; Moubaraki, B.; Murray, K. S. *Chem. Commun.* **1998**, 439–440.

(10) Chow, Y. M.; Britton, D. *Acta Crystallogr., Sect. B: Struct. Sci.* **1975**, *31*, 1934.

(11) Shi, Y. J.; Chen, X. T.; Li, Y. Z.; Xue, Z.; You, X. Z. *New J. Chem.* **2002**, *26*, 1711–1713.

(12) (a) Jensen, P.; Batten, S. R.; Fallon, G. D.; Hockless, D. C. R.; Moubaraki, B.; Murray, K. S.; Robson, R. *J. Solid State Chem.* **1999**, *145*, 387–393. (b) Jensen, P.; Batten, S. R.; Fallon, G. D.; Moubaraki, B.; Murray, K. S.; Price, D. J. *Chem. Commun.* **1999**, 177–178.

(13) (a) Drew, M. G. B.; Prasad, R. N.; Sharma, R. P. *Acta Crystallogr., Sect. C: Cryst. Struct. Commun.* **1985**, *41*, 1755–1758. (b) Iida, K.; Oonishi, I.; Nakahara, A.; Komoyama, Y. *Bull. Chem. Soc. Jpn.* **1970**, *43*, 2347–2354.

(14) *SAINT, version 6.02; SADABS, version 2.03;* BrukerAXS, Inc.: Madison, WI, 2002.

(15) Sheldrick, G. M. *SHELXS 97, Program for Structure Solution;* University of Göttingen: Germany, 1997.

(16) Sheldrick, G. M. *SHELXL 97, Program for Crystal Structure Refinement;* University of Göttingen: Germany, 1997.

(17) Spek, A. L. *J. Appl. Crystallogr.* **2003**, *36*, 7–13.

(18) Farrugia, L. J. *J. Appl. Crystallogr.* **1997**, *30*, 565.

(19) Farrugia, L. J. *J. Appl. Crystallogr.* **1999**, *32*, 837–838.

(20) Addison, A. W.; Rao, T. N.; Reedjik, J.; Rijn, J. V.; Verschoor, C. G. *J. Chem. Soc., Dalton Trans.* **1984**, 1349–1356.

(21) (a) Shi, Z.; Peng, J.; Gómez-García, C. J.; Benmansour, S.; Gu, X. *J. Solid State Chem.* **2006**, *179*, 253–265. (b) Gómez-García, C. J.; Coronado, E.; Borrás-Almenar, J. J. *Inorg. Chem.* **1992**, *31*, 1667–1673. (c) Lloret, F.; Julve, M.; Cano, J.; Ruiz-García, R.; Pardo, E. *Inorg. Chim. Acta* **2008**, *361*, 3432–3445. (d) Mosconi, E.; Yum, J. H.; Kessler, F.; Gómez García, C. J.; Zuccaccia, C.; Cinti, A.; Nazeeruddin, M. K.; Grätzel, M.; De Angelis, F. *J. Am. Chem. Soc.* **2012**, *134*, 19438–19453.

(22) Lines, M. E. *J. Chem. Phys.* **1971**, *55*, 2977–2984.

(23) Tsukerblat, B.; Palii, A.; Mirovitskii, V. Y.; Ostrovsky, S. M.; Turta, K.; Jovmir, T.; Shova, S.; Bartolome, J.; Evangelisti, M. *J. Chem. Phys.* **2001**, *115*, 9528–9535.

(24) Palii, A.; Tsukerblat, B.; Clemente-Juan, J. M.; Coronado, E. *Int. Rev. Phys. Chem.* **2010**, *29*, 135–230.

(25) (a) Borrás-Almenar, J. J.; Clemente-Juan, J. M.; Coronado, E.; Tsukerblat, B. S. *Inorg. Chem.* **1999**, *38*, 6081–6088. (b) Borrás-Almenar, J. J.; Clemente-Juan, J. M.; Coronado, E.; Tsukerblat, B. S. *J. Comput. Chem.* **2001**, *22*, 985–991.

(26) (a) Ruiz, E.; Alemany, P.; Alvarez, S.; Cano, J. *J. Am. Chem. Soc.* **1997**, *119*, 1297–1303. (b) Ruiz, E.; Alvarez, S. *Chem. Commun.* **1998**, 2767–2768.

(27) (a) Tao, R.; Mei, C.; Zang, S.; Wang, Q.; Niu, J.; Liao, D. *Inorg. Chim. Acta* **2004**, *357*, 1985–1990. (b) Tao, R.; Li, F.; Zang, S.; Cheng, Y.; Wang, Q.; Niu, J.; Liao, D. *J. Coord. Chem.* **2006**, *59*, 901–909.

(28) Nesterov, D. S.; Kokozay, V. N.; Skelton, B. W.; Jezierska, J.; Ozarowski, A. *Dalton Trans.* **2007**, 558–564.